World Applied Sciences Journal 20 (7): 965-975, 2012
ISSN 1818-4952

DOI: 10.5829/idosi.wasj.2012.20.07.1609

Application of Pomegranate (*Punica granatum*) Pulp as a New Biosorbent for the Removal of a Model Basic Dye (Methylene Blue)

[1]Fuat Güzel, [2]Önder Aksoy and [1]Gülbahar Akkaya

[1]Department of Chemistry, Faculty of Education, Dicle University, 21280 Diyarbakir, Turkey
[2]Instute of Science Technologies, Dicle University, 21280 Diyarbakir, Turkey

Abstract: The biosorption of methylene blue (MB) as a model adsorbent from aqueous solution using new biosorbent prepared from pomegranate pulps (PP) has been investigated. Batch studies were performed to evaluate and optimize the effects of various parameters such as contact time, initial dye concentration, solution pH, adsorbent dosage, temperature and ionic strength. The biosorption kinetic was tested by pseudo-first order, pseudo-second order and intraparticle diffusion models. Kinetic studies indicated that the pseudo-second order model fitted to the experimental data well. The equilibrium behavior of MB adsorption at different temperatures was examined by the Langmuir and Freundlich isotherm models. The equilibrium sorption was best described by the Langmuir isotherm model. The maximum monolayer sorption capacity of PP for MB was found to be 36.36, 28.74 and 26.67 mg g^{-1} at 30, 40 and 50°C, respectively. The thermodynamic studies indicated that the biosorption reactions were spontaneous and exothermic. Characterization of the PP was performed using Fourier Transform Infrared Spectroscopy (FTIR). Desorption experiments were also conducted to examine the recycling use capacity with different desorbents. According to the experimental results, PP seems to be an effective, low-cost and alternative adsorbent precursor for the removal of MB from aqueous solutions.

Key words: Biosorption · Pomegranate Pulp · Methylene Blue · Kinetics · Thermodynamics

INTRODUCTION

Most of the industries in many countries, i.e. textiles, paper, plastics, leather, food, cosmetics, etc., use dyes or pigments to color their final product. Dyes present in waste water may cause serious environmental pollution problems, in the form of reduced light penetration and reduced photosynthesis [1].

The used common dye removal techniques, such as chemical coagulation/ flocculation, ozonation, oxidation processes, chemical precipitation, ion exchange, reverse osmosis, ultra-filtration etc., for the removal of dyes from dye containing wastewater have serious restrictions such as high cost, formation of hazardous by-products or intensive energy requirements [2, 3]. Therefore, the development of efficient, low-cost and environmentally friendly technologies to reduce dye content in wastewater is extremely necessary. Recently, many researchers have attempted to use alternative low-cost sorbents to substitute activated carbons. Some of these alternative biosorbents are Pinus brutia Ten [3], beech sawdust [4], cupuassu shell [5], pineapple leaf powder [6], peanut husk [7], jackfruit leaf powder [8], palm oil mill effluent [9], poplar sawdust [10], citrus fruit peel [11], Brazil nut shells [12], marine Aspergillus wentii [13], tea wastages [14] etc., there is lack of information about the sorption ability of Pomegranate (*Punica granatum*) pulp (PP), an abundantly available waste products. The Turkey's pomegranate production and exports, is third after from the India and Iran's in the world rankings.

In this study, pomegranate pulp (PP) evaluated as a new biosorbent for removal of a basic dye from aqueous from the solution. We chose in this study Methylene Blue as a model compound because of its strong adsorption study on solids and its use in characterizing adsorptive materials. MB is the most commonly used substance for dying natural fibers as cotton or silk. It can cause eye burns by direct contact and nausea, vomiting, profuse sweating, mental confusion and methemoglobinemia by ingestion [15]. We examined the effects of solution pH, biosorbent dose, contact time, dye initial concentration, temperature and ionic strength on the MB biosorption

Corresponding Author: Dr. Fuat Güzel, Department of Chemistry, Faculty of Education, Dicle University, 21280 Diyarbakir, Turkey. Tel: +90-412 2488377

process onto PP from aqueous solution. FTIR analysis was carried out to understand the surface functional groups of PP. Equilibrium data were analyzed by Langmuir and Freundlich isotherm models. Kinetic data were evaluated by pseudo-first order, pseudo-second order and intraparticle diffusion models. Thermodynamic parameters such as free energy (ΔG), enthalpy (ΔH) and entropy (ΔS) were also determined. Desorption studies were carried out with distilled water and various acid solutions.

MATERIALS AND METHODS

Preparation and Characterization of Biosorbent: The raw PP was collected from Limkon fruit juice factory in Adana, East-South Anatolia region, Turkey and it was used as an adsorbent. They were firstly washed with distilled water, dried at 70 °C for 24 h, crushed in a grinder and sieved to obtain particle size in the range of 500 μm. The powdered biosorbent was stored in desiccators until use. No other physical or chemical treatments were given prior to adsorption experiments.

pH_{PZC} of PP was determined by the solid addition method, as described by Preethi and Sivasamy [16]. A series of 50 mL of 0.01M NaCl solution was placed in a closed erlenmeyer flask. The pH was adjusted to a value between 2 and 12 by adding 0.1M HCl or 0.1M NaOH solution. Then 0.15 g of each PP sample was added and agitated at 120 rpm for 48 h under atmospheric conditions. The final pH measured and the results were plotted with ?pH (Initial pH-Final pH) against final pH. The pH_{PZC} is the point where the curve pH_{final} versus $pH_{initial}$ crosses the line $pH_{initial} = pH_{final}$ (Fig. 1). From Fig. 1, pH_{PZC} of PP was found to be 6.53.

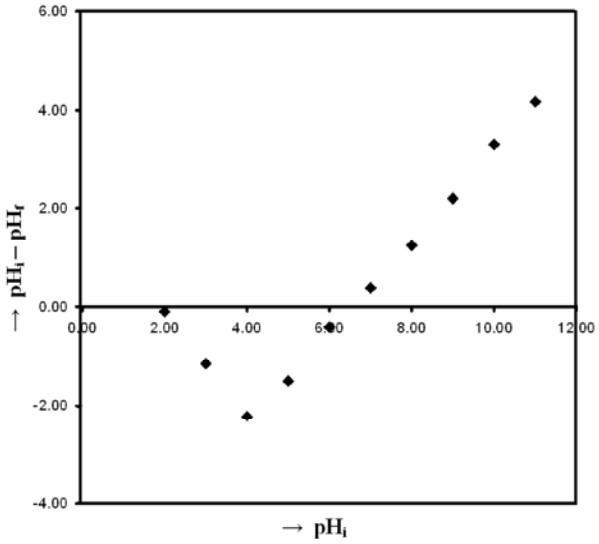

Fig. 1: Determination of pH_{PZC} for PP

The FTIR spectrums of PP before and after the adsorption of MB were taken to determine the frequency changes in the functional groups of the adsorbent and compared with each other to confirm the adsorption of MB (Fig. 2). The spectra were recorded from 4000-400 cm^{-1}.

Preparation of Dye Solutions: MB (type: cationic, nature: basic; C.I number: 52015; Molecular formula: $C_{16}H_{18}N_3SCl$; Molecular weight: 313.9; λ_{max}: 660 nm) was purchased supplied by Sigma-Aldrich. Stock solution was prepared by dissolving 2.0 g of MB in 1 L distilled water. The experimental solutions were obtained by diluting the dye stock solution (2000 ppm) to the desired concentrations.

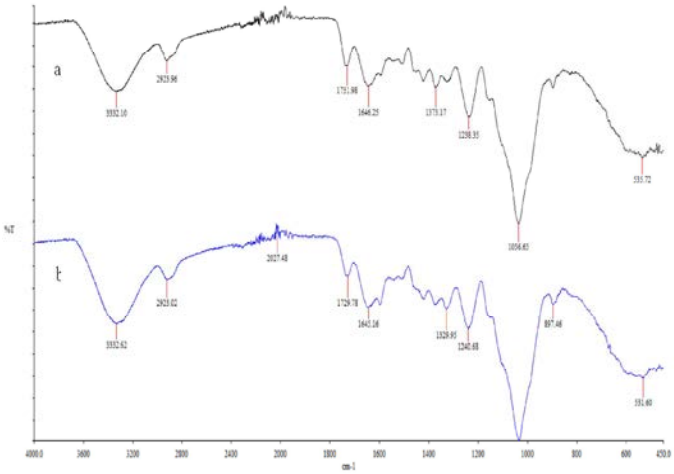

Fig. 2: FTIR spectrums of PP: (a) raw PP (b) MB loaded PP

Batch Biosorption Experiments: Biosorption experiments were carried out in 100 ml flasks and the total volume of the reaction solution was kept at 50 ml. The flasks were shaken at 150 rpm for the required time in a water bath shaker. The experiments were carried out by varying the contact time from 5 to 300 min, the biosorbent dosage from 0.1 to 1.0 g/L, the pH from 2 to 11, the initial concentration from 25 to 300 mg/L and the temperature from 30 to 60 °C. The temperature was controlled using an isothermal shaker. After each biosorption process, the samples were centrifuged (5000 rpm, 10 min) for solid-liquid separation and the residual dye concentration in solution was analyzed by a UV-vis spectrophotometer (Perkin Elmer, Lamda 25) at 665 nm. The amount of dye adsorbed onto per gram of adsorbent (q_e) and the percentage adsorption efficiency (A %)) were calculated using Eqs. (1) and (2), respectively.

$$q_e = \frac{(C_0 - C_e)V}{m} \quad (1)$$

$$A\% = \frac{C_0 - C_e}{C_0} 100 \quad (2)$$

where C_0 and C_e are initial and equilibrium MB concentrations, respectively (mg/L), V is MB solution volume (L), m is the mass of adsorbent (g).

Desorption studies were carried out with 0.1 M of different desorbent agents such as distillated water, HCl, HNO_3, H_3PO_4, CH_3COOH and citric acid. The desorption efficiency (D %) was calculated using Eq. (3).

$$D\% = \frac{m_d}{m_a} x100 \quad (3)$$

where m_d is the amount of MB desorbed (mg/L), m_a is the amount of MB adsorbed (mg /L).

RESULTS AND DISCUSSION

Characterization of the PP

FTIR Analysis: The results of FT-IR analysis indicated that carbonyl and hydroxyl groups were included on the surface of the PP (Fig. 2). The peaks at 3332 cm^{-1} indicate O-H stretching vibrations and spectra bands observed at 2923 cm^{-1} represent vibration of aliphatic C-H especially due to C-CH and C-CH_2 bonds. The peaks at 1731 and 1646 cm^{-1} corresponds to stretching vibrations of C=O. The peaks observed at 1373 cm^{-1} and 1238 cm^{-1} were assigned to the in-plane bending vibration of C-H bond in methyl groups and bending vibration of O-H, respectively. The peak at 1036 cm^{-1} indicates C-O stretching vibration of carboxylic acid. The infrared spectrums of PP before and after adsorption of MB were examined. No important difference was seen between the spectra, which indicate that physical adsorption was the predominant mechanism in the adsorption process.

Studies on Optimum Biosorption Conditions

pH_{pzc} and Effect of Solution pH: The effect of pH on the amount of MB adsorbed onto PP was investigated over the pH range from 2.0 to 11.0. The pH was adjusted using 0.1 mol/L NaOH or 0.1 mol/L HCl solutions. Fig. 3a shows the effect of initial solution pH on the biosorption of MB onto PP. It was observed that a sudden increase in amount of MB adsorbed from 5.36 to 20.68 mg/g, occurred when the pH values changed from 2.0 to 7.0. This can be on the basis of a decrease in competition between positively charged H^+ and MB for surface sites and also by decrease in positive surface charge on the adsorbent, which results in a lower electrostatic repulsion between the surface and MB. The effect of pH can also be explained in terms of the zero point of charge (pH_{pzc}) of the adsorbent. From Fig. 1, the point of zero charge (pH_{PZC}) for PP was found to be 6.53. The surface charge of the adsorbent is positive at pH< pH_{pzc}, while it is negative at pH> pH_{pzc} [17]. Thus, below pH 6.53, PP was positively charged and did not favor adsorption of positively charged MB due to electrostatic repulsion. The optimum pH for MB biosorption onto PP was found to be in the range 7.0-10.0 (Fig. 3a), which was higher than the pH_{pzc} value of 6.53. Thus, the PP acts as a negative surface and attracts the cationic MB. A similar behavior has been reported by other MB biosorption studies [18, 19]. Moreover, the decrease in adsorption at pH higher from pH 10 values might be due to hydrolysis, of PP itself which creates positively charged sites. Similar results have been reported by other some researchers [20, 21]. Therefore, pH 7 was selected to be the optimum pH for further studies.

Effect of Contact Time and Initial Dye Concentration: Biosorption experiments were carried out for different contact time at initial dye concentration with a fixed adsorbent dosage of 0.1 g/50 mL at pH 7. The results are presented in Fig. 3b. Figure shows the progress of MB adsorption versus the contact time and different concentrations of MB on PP at 30 °C. It was observed that the adsorption process can be divided into three stages. The first stage was the rapid initial adsorption within 60 min. The following stage was slow adsorption process within the range of 60-90 min; the increase of adsorption capacity became much slower than that of first stage.

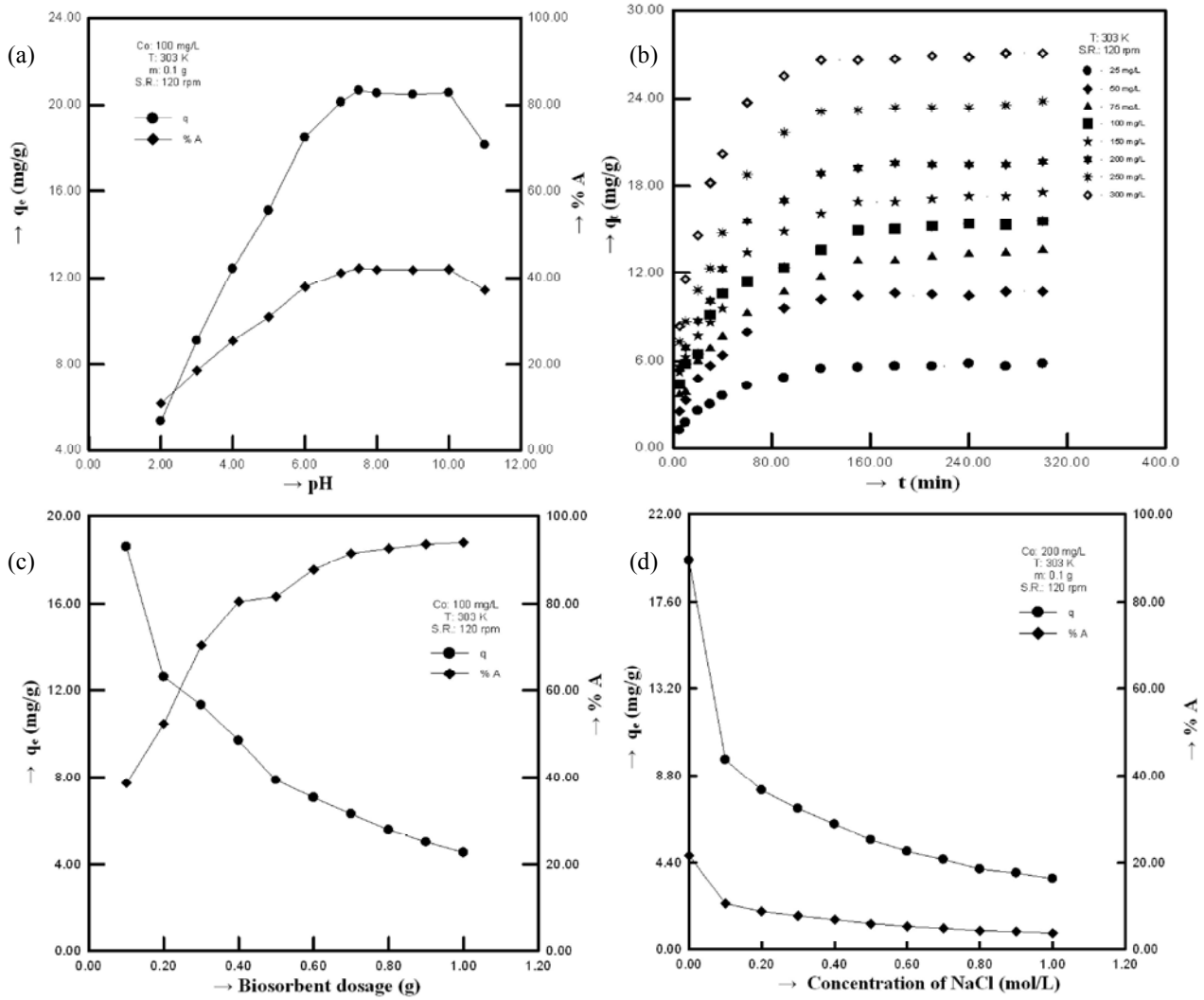

Fig. 3: Effect of a) solution pH, b) contact time and initial dye concentration, c) biosorbent dose, d) ionic strength

Finally, the adsorption capacity did not vary significantly after 150 min, the adsorption would be in a state of dynamic equilibrium between the dye desorption and adsorption. The removal of MB by adsorption on PP was found to increase with time and attained a maximum value at 150 min. It was evident from the Fig. 3b that adsorption equilibrium was established at 150 min. And 150 min was seen as the adsorption equilibrium time for all other experiments.

The value of q increased from 5.71 to 26.88 mg/g with increasing from 25 to 300 mg/L of the initial dye concentration. This is probably due to the mass transfer driving force become larger and the interaction between MB and adsorbent was enhanced, hence resulting in higher adsorption capacity. Similar results have been reported by other some researchers [22, 23].

Effect of Biosorbent Dose: The adsorption of MB onto PP was studied by varying the adsorbent quantity (0.1-1.0 g/L) in solution while keeping the initial dye concentration (100 mg/L), temperature (303 K) and pH 7 constant for 150 min equilibrium time. The values of q_e and A % at different dose of PP were presented in Fig. 3c. The removal percentage of MB increased from 38.6 % to 94.0 % for biosorbent dosage of 0.1 and 1.0 g/L, respectively. This is due to the availability of more binding sites as the dose of biosorbent increased. However, the amount of MB adsorbed onto the sorbent, q (mg/g), was found to decrease from 18.6 to 4.53 mg/g with increasing biosorbent dose. It is due to the high number of unsaturated biosorption sites during biosorption process. Similar results were previously reported by some researchers [24-27].

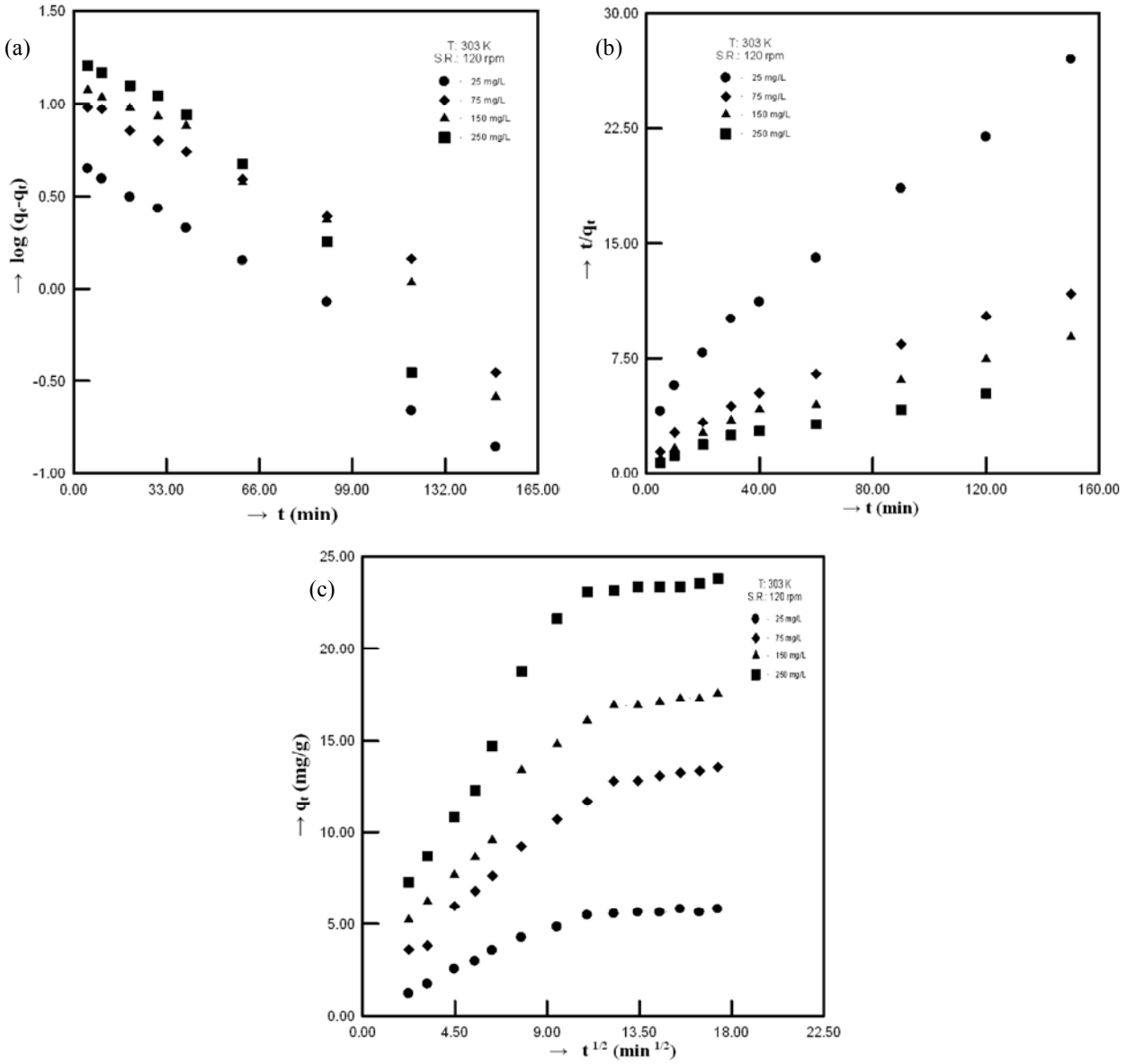

Fig. 4: (a) Pseudo-first-order (b) Pseudo-second-order, (c) intraparticle diffusion kinetic plots for biosorption of MB onto PP at different initial concentrations

Effect of Salt Ionic Strength: In dyeing processes, NaCl is often used as a stimulator, leading to higher salt concentration in the dye wastewater [28]. It was important to discuss the effect of salt ionic strength on the adsorption of MB onto PP because dyeing wastewater usually contains high salt concentration. Fig. 3d shows the effect of the concentration of NaCl on the biosorption of MB by PP. The removal efficiency decreased from 21.67 to 3.96 % with an increase in salt concentration from 0 to 1.0 mol/L. This indicated that the biosorption decreased as the NaCl concentration increased, which may be due to the competitive effect between MB ions and cations from the salt for the sites available for sorption. Similar observations were observed in the studies of some researchers [23, 28, 29].

Kinetic Data Analysis: Three simplified kinetic models namely pseudo-first-order, pseudo-second-order and intraparticle diffusion models have been discussed to identify the rate and kinetics of sorption of MB on prepared PP adsorbent.

Pseudo-First-Order Model: The Lagergren's rate equation [30] is one of the most widely used rate equation to describe the adsorption of an adsorbate from the liquid phase. A linear form of the pseudo first-order kinetic model is represented as Eq. (4):

$$\log(q_e - q_t) = \log q_e - \left(\frac{k_1}{2.303}\right)t \quad (4)$$

where q_e and q_t (mg/g) are the amounts of adsorbed MB at equilibrium and at time t, respectively, k_1 (1/min) is pseudo-first-order rate constant and t (min) is contact time. The slopes and intercept of log (q_e-q_t) versus t plot (Fig. 4a) were used to determine the first order rate constants (k_1) and q_e(cal), compiled in Table 1 along with correlation coefficients (R^2) values.

Pseudo-Second-Order Model: Adsorption kinetic was explained by the pseudo second-order model given by Ho *et al*. [31]. A linear form of the pseudo second-order kinetic model is represented as Eq. (5):

$$\frac{t}{q_t} = \frac{1}{k_2 q_e^2} + \frac{t}{q_e} \quad (5)$$

where k_2 is the pseudo-second-order rate constant (g mg^{-1} min^{-1}). According to Eq. (6), a plot of q_t versus $t^{1/2}$ should be a straight line with a slope k_{id} and intercept C The slopes and intercept of t/q_t vs t plot were used to determine the first order rate constants (k_2) and q_e(cal) (Fig. 4b), compiled in Table 1 along with correlation coefficients (R^2) values.

As can be seen from Table 1, the correlation coefficients (R^2) obtained from pseudo second-order model were found to be higher than 0.98 for all concentrations, which were larger than those of the pseudo-first-order model. The results revealed that the pseudo second-order model was the best one in describing the kinetics of MB adsorbed onto PP. On the other hand, the calculated values of $q_{e,cal}$ obtained from the pseudo second-order model perfectly agreed with the experimental values of $q_{e,exp}$ at four initial concentrations, respectively. However, the $q_{e,cal}$ obtained from the pseudo first-order model were much lower than the $q_{e,exp}$. Consequently, the adsorption of MB from aqueous solution onto PP followed the pseudo second-order model well.

Intraparticle Diffusion Model: Kinetic data was further analyzed using the intraparticle diffusion model based on the theory proposed by Weber and Morris [32]. A linear form of the Weber and Morris kinetic model is represented as Eq. (6):

$$q_t = k_{id} t^{1/2} + C \quad (6)$$

where k_{id} is the intraparticle diffusion rate constant (mg g^{-1} $min^{-1/2}$) and C is a constant related to the thickness of the boundary layer. According to Eq. (6), a plot of q_t versus $t^{1/2}$ should be a straight line with a slope k_{id} and intercept C when the adsorption mechanism follows the intraparticle diffusion process. As can be seen from Fig. 4c, the intercept of the line does not pass through the origin and the R^2 are less than 0.99 suggesting that two or more steps are involved in the MB adsorption onto the prepared adsorbent. The deviation of straight line in Weber and Morris model may be due to difference in the rate of mass transfer in the initial and final stages of adsorption. Similar results have been reported by other some researchers [33]. The values of k_{id} and C obtained

Table 1: Kinetic parameters for MB removal onto PP at different initial concentrations (T: 303 K; pH: 7; adsorbent mass: 0.1 g)

		Pseudo-first-order			Pseudo-second-order		
C_o (mg/L)	$q_{e,exp}$ (mg/g)	$q_{e,cal}$ (mg/g)	k_1 (1/min)	R^2	$q_{e,cal}$ (mg/g)	$k_2 x 10^3$ (g/mg min)	R^2
25	-------	5.42	0.0242	0.9593	6.65	4.90	0.9916
75	-------	11.94	0.0205	0.9524	14.64	2.34	0.9819
150	-------	16.50	0.0249	0.9664	19.65	1.80	0.9835
250	35.38	24.84	0.0320	0.9593	27.47	1.37	0.9867

Table 2: The intraparticle diffusion constants for the adsorption of MB onto PP at different initial concentrations (T: 303 K; pH: 7; adsorbent mass: 0.1 g)

C_o (mg/L)	$k_{id,1}$(g/mg)	C_1	R^2_1	$k_{id,1}$ (g/mg)	C_2	R^2_2	$k_{id,3}$ ($min^{½}$)	C_3	R^2_1
25	0.5538	0.009	0.9979	0.2608	2.445	0.8575	0.0369	5.142	0.9336
75	1.0633	0.969	0.9685	0.7878	3.336	0.9970	0.1562	10.821	0.9648
150	1.0584	2.895	0.9994	0.8398	6.878	0.9997	0.1249	15.306	0.9834
250	2.0230	2.175	0.9741	0.9932	12.215	0.9998	0.1049	21.875	0.9112

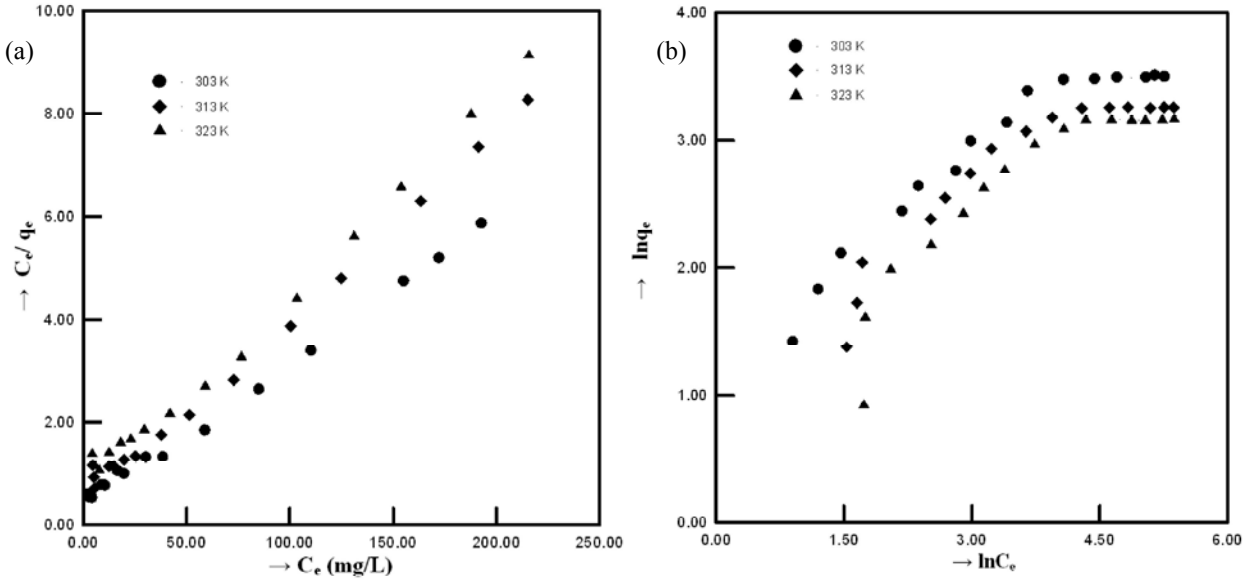

Fig. 5: (a) Langmuir, (b) Freundlich isotherm plots for different temperatures on the biosorption of MB by PP

from the second stage linear regression analysis were listed in Table 2. It was observed that with the increasing initial MB concentration from 25 to 250 mg/L, the values of C increased from 5.28 to 27.96, which reflected the increase in the thickness of boundary layer and the decrease in the chance of external mass transfer. Hence the chance of internal mass transfer was increased and the decrease in the chance of external mass transfer. Similar observations were observed in the studies of some researchers [23, 34].

Isotherm Data Analysis: The adsorption isotherm studies were carried out at different temperatures from 20 to 60 °C. The isotherm data obtained were analyzed with the Langmuir and Freundlich isotherm models.

Langmuir Model: The Langmuir model is obtained on the basis of the ideal assumption that all the adsorption sites are energetically identical (monolayer adsorption) and adsorption occurs on a structurally homogeneous adsorbent [35]. A linear form of the Langmuir isotherm model for solid/liquid systems is represented as Eq. (7):

$$\frac{C_e}{q_e} = \frac{1}{q_m b} + \frac{C_e}{q_m} \tag{7}$$

where C_e (mg/L) and q_e (mg/g) are the residual dye concentration and the amount of dye adsorbed per gram of adsorbent at equilibrium, respectively, q_m (mg/g) is the monolayer adsorption saturation capacity, b (L/mg) is a Langmuir constant relating to adsorption energy. Hence, a plot of C_e/q_e vs C_e (Fig. 5a) should be a straight line with a slope ($1/q_m$) and an intercept as ($1/q_m b$). The values of constants q_m and b were calculated and reported in Table 3. The maximum monolayer capacity q_m obtained from the Langmuir equation at 30 °C is 36.36 mg/g The constants q_m and K_L decreased with increasing temperature, indicating that the adsorption density was lower and the adsorption energy lower, at higher temperatures. Table 4 lists a comparison of maximum monolayer adsorption capacity of MB on various adsorbents.

Freundlich Model: The Freundlich model can be applied for non-ideal sorption on heterogeneous surfaces and multilayer sorption [36]. A linear form of the Freundlich isotherm for solid/liquid systems is represented as Eq. (8):

$$\log q_e = \log K_F + \frac{1}{n}\log C_e \tag{8}$$

where K_F [(mg/g) (mg/L)$^{-1/n}$] is a constant for the system, related to the bonding energy. K_F can be defined as the adsorption or distribution coefficient and represents the quantity of dye adsorbed onto adsorbent for unit equilibrium concentration. 1/n is indicating the adsorption intensity of dye onto the adsorbent or surface heterogeneity, becoming more heterogeneous as its value gets closer to zero. A value for 1/n below 1 indicates a normal Langmuir isotherm, while 1/n > 1 is indicative of cooperative adsorption. This model deals with the multilayer adsorption of the substance on the adsorbent.

Table 3: Freundlich and Langmuir isotherm constants for biosorption of MB onto PP at different temperatures

Temperature	Freundlich			Langmuir		
(K)	K_F [(mg/g)(L/mg)$^{1/n}$]	1/n	R^2	q_m (mg/g)	b (L/mg)	R^2
303	4.20	0.445	0.9051	36.36	0.063	0.9963
313	3.48	0.427	0.8476	28.74	0.060	0.9942
333	2.31	0.493	0.8242	26.67	0.047	0.9926

Table 4: Comparison of sorption capacity of PP for MB with other agro-based waste sorbents

Adsorbent	q_m (mg/g)	References
Peanut husk	72.13	[7]
Jackfruit leaf powder	252.83	[8]
Palm oil mill effluent	66.23	[9]
Poplar sawdust	4.34	[10]
Brazil nut shells	7.81	[12]
Rice husk	40.58	[18]
Posidonia oceanica (L.) fibres	5.56	[19]
Meranti sawdust	120.48	[20]
Broad bean peels	192.7	[21]
Lotus leaf	221.70	[23]
Softstem bulrush	53.8	[28]
Phoenix tree's leaves	89.7	[29]
Pomegranate Pulp	36.36	This study

Table 5: Thermodynamic parameters for biosorption of MB onto PP

T (K)	ΔG (kJ/mol)	ΔH (kJ/mol)	ΔS (J/mol K)
303	-7.69 -11.87	-13.93	
313	-7.56		
333	-7.28		

The values of K_f and 1/n were calculated from the intercept and slope of the plot of log q_e versus log C_e (Fig. 5b and Table 3). As seen from the Table 3, 1/n is <1, indicating that MB is favorably adsorbed by PP.

From the correlation coefficients (R^2) reported in Table 3, the Langmuir adsorption isotherm model yielded best fit as indicated by the highest R^2 values (>0.99) at all temperatures compared to the Freundlich model.

Biosorption Thermodynamic: The thermodynamic data reflect the feasibility and spontaneous nature of adsorption process. The parameters such as ΔG, ΔH and ΔS can be estimated by equilibrium constants changing with temperature. The ΔG (kJ mol^{-1}) of adsorption reaction is given by:

$$\Delta G = -RT \ln b \quad (9)$$

where, R is the universal gas constant (8.314 J mol^{-1} K^{-1}), T shows the absolute temperature (K). The values of ΔH and ΔS can be calculated from the Van't Hoff equation:

$$\ln b = -\frac{\Delta H}{RT} + \frac{\Delta S}{RT} \quad (10)$$

According to Eq. (10), the value of ΔH and ΔS was obtained from the slope and the intercept from the linear plot of lnK_L versus 1/T, respectively. The calculated thermodynamic parameters were summarized in Table 5. The obtained values for ΔG are-7.56,-7.69 and?7.28 kJ mol^{-1} for MB biosorption on GP at 30, 40 and 50°C, respectively. Because all ΔG values are negative, the adsorption of MB onto GP is a spontaneous process, confirming the affinity of GP for the MB. Generally, a value of ΔG in between 0 and -20 kJ/mol is consistent with electrostatic interaction between adsorption sites and the adsorbing ion (physical adsorption) while a more negative ΔG value ranging from -80 to -400 kJ/mol indicates that the adsorption involves charge sharing or transferring from the adsorbent surface to the adsorbing ion to form a coordinate bond (chemisorption) [37]. The magnitude of ΔG in the range of -7.28 to -7.69 kJ/mol was shown. These values suggest that the adsorption is a typical physical process. The ΔH parameter is-11.87 kJ mol^{-1} for MB biosorption on PP. The negative ΔH is an indicator of exothermic nature of the biosorption involving weak attractive. The ΔS parameter is-13.93 kJ mol^{-1}K^{-1} for MB biosorption on PP.

The negative ΔS value confirms the decreased randomness at the PP-MM interface during biosorption. The low value of ΔS also indicates that no remarkable change on entropy occurs.

Desorption Studies: Desorption experiments was conducted to regenerate the adsorbent and to recover the dye. The MB desorption efficiency with 0.1 M solutions of different desorbent agents (H_2O, HCl, HNO_3, H_3PO_4,CH_3COOH and citric acid) was investigated. the desorption efficiency of MB was determined as 78.25% with citric acid, 57.81% with Hcl, 55.73% with HNO_3, 68.64% with H_3PO_4, 54.81% with CH_3COOH and 3.29% with H_2O. It was observed that the desorption percentages of MB with distilled water were too low. MB was desorbed by citric acid with high percentages when compared with other desorbent agents. There are three carboxyl groups in the structure of citric acid, which means more binding sites than other acids. Due to the number of carboxyl groups in the structure of citric acid, this resulted in increasing the effectiveness of citric acid.

CONCLISONS

In this study, PP as a natural biosorbent was investigated for the removal of MB from aqueous solution in the batch mode. The bisorption capacity was affected by various parameters including contact time, adsorbent dose, initial MB concentration, solution pH, salt ionic strength and temperature. The equilibrium data were well fitted to Langmuir isotherm model. The monolayer sorption capacities of PP for MB were 36.36, 28.74 and 26.67 mgg^{-1} at different temperatures 303, 313 and 323 K, respectively. Kinetic studies showed that the biosorption process followed the pseudo-second-order model. The thermodynamic calculations indicated the feasibility, exothermic and spontaneous nature of the biosorption process at 30-50 °C. Sodium chloride caused a decrease in the sorption potential of the biosorbent. A large number of carbonyl and hydroxyl groups were observed on the surface of the PP by FTIR analysis. Among used desorbents, the highest desorption efficiency was obtained with citric acid.

ACKNOWLEDGEMENTS

The authors acknowledge the Scientific Research Fund of Dicle University for financial support [Project No: 11-ZEF-38].

REFERENCES

1. Özer, D., G. Dursun and A. Özer, 2007. Methylene blue adsorption from aqueous solution by dehydrated peanut hull, J. Hazard. Mater., 144: 171-179.
2. Banat, I.M., P. Nigam, D. Singh and R. Marchant, 1996. Microbial decolorization of textile dye containing effluents: a review, Bioresour. Technol., 58: 217-227.
3. Deniz, F., S. Karaman and S.D. Saygıdeğer, 2011. Biosorption of a model basic dye onto Pinus brutia Ten.: Evaluating of equilibrium, kinetic and thermodynamic data, Desalination, 270: 199-205.
4. Witek-Krowiak, A., 2011. Analysis of influence of process conditions on kinetics of malachite green biosorption onto beech sawdust, Chem. Eng. J., 171: 976-985.
5. Cardoso, N.F., E.C. Lima, I.S. Pinto, C.V. Amavisca, B. Royer, R.B. Pinto, W.S. Alencar and S.F.P. Pereira, 2011. Application of cupuassu shell as biosorbent for the removal of textile dyes from aqueous solution, J. Environ. Manage., 92: 1237-1247.
6. Chowdhury, S., S. Chakraborty and P. Saha, 2011. Biosorption of Basic Green 4 from aqueous solution by Ananas comosus (pineapple) leaf powder, Colloids Surf., B, 84: 520-527.
7. Song, J., W. Zou, Y. Bian, F. Su and R. Han, 2011. Adsorption characteristics of methylene blue by peanut husk in batch and column modes, Desalination, 265: 119-125.
8. Uddin, Md. T., Md. Rukanuzzaman, Md. M.R. Khan and Md. A. Islam, 2009. Adsorption of methylene blue from aqueous solution by jackfruit (Artocarpus heteropyllus) leaf powder: A fixed-bed column study, J. Environ. Manage., 90: 3443-3450.
9. Gobi, K., M.D. Mashitah and V.M. Vadivelu, 2011. Adsorptive removal of Methylene Blue using novel adsorbent from palm oil mill effluent waste activated sludge: Equilibrium, thermodynamics and kinetic studies, Chem. Eng. J., 171: 1246-1252.
10. Pekkuz, H., I. Uzun and F. Güzel, 2008. Kinetics and thermodynamics of the adsorption of some dyestuffs from aqueous solution by poplar sawdust, Bioresour. Technol., 99: 2009-2017.
11. Dutta, S., A. Bhattacharyya, A. Ganguly, Samya Gupta and S. Basu, 2011. Application of Response Surface Methodology for preparation of low-cost adsorbent from citrus fruit peel and for removal of Methylene Blue, Desalination, 275: 26-36.

12. De Oliveira Brito, S.M., H.M.C. Andrade, L.F. Soares and R.P. de Azevedo, 2010. Brazil nut shells as a new biosorbent to remove methylene blue and indigo carmine from aqueous solutions, J. Hazard. Mater., 174: 84-92.
13. Khambhaty, Y., K. Mody and S. Basha, 2012. Efficient removal of Brilliant Blue G (BBG) from aqueous solutions by marine Aspergillus wentii: Kinetics, equilibrium and process design, Ecol. Eng., 41: 74-83.
14. Giahi, M., R. Rakhshaee and M.A. Bagherinia, 2011. Removal of methylene blue by tea wastages from the synthesis waste waters, Chin. Chem. Lett., 22: 225-228.
15. Rafatullah, M., O. Sulaiman, R. Hashim and A. Ahmad, 2010. Adsorption of methylene blue on low-cost adsorbents: a review, J. Hazard. Mater., 177: 70-80.
16. Preethi, S. and A. Sivasamy, 2006. Removal of safranin basic dye from aqueous solutions by adsorption onto corncob activated carbon, Ind. Eng. Chem. Res., 45: 7627-7632.
17. You, Z., L. Wang and J. Qi, 2009. Biosorption of methylene blue from aqueous solution using a bioenergy forest waste: Xanthoceras sorbifolia seed cost, Clean, 37(8): 642-648.
18. Vadivelan, V. and K.V. Kumar, 2005. Equilibrium, kinetics, mechanism and process design for the sorption of methylene blue onto rice husk, J. Colloid Interface Sci., 286: 90-100.
19. Ncibi, M.C., B. Mahjoub and M. Seffen, 2007. Kinetic and equilibrium studies of methylene blue biosorption by *Posidonia oceanica* (L.) fibres, J. Hazard. Mater., 139: 280-285.
20. Ahmad, A., M. Rafatullah, O. Sulaiman, M.H. Ibrahim and R. Hashim, 2009. Scavenging behaviour of meranti sawdust in the removal of methylene blue from aqueous solution, J. Hazard. Mater., 170: 357-365.
21. Hameed, B.H. and M.I. El-Khaiary, 2008. Sorption kinetics and isotherm studies of a cationic dye using agricultural waste: broad bean peels, J. Hazard. Mater., 154: 639-648.
22. Tan, I.A.W., A.L. Ahmad and B.H. Hameed, 2008. Adsorption of basic dye on high-surface area activated carbon prepared from coconut husk: equilibrium, kinetic and thermodynamic studies, J. Hazard. Mater., 154: 337-346.
23. Han, X., W. Wang and X. Ma, 2011. Adsorption characteristics of methylene blue onto low cost biomass material lotus leaf, Chem. Eng. J., 171: 1-8.
24. Mall, I.D., V.C. Srivastava and N.K. Agarwal, 2006. Removal of Orange-G and Methyl Violet dyes by adsorption onto bagasse fly ash-kinetic study and equilibrium isotherm analyses, Dyes Pigments, 69: 210-223.
25. Yu, L.J., S.S. Shukla, K.L. Dorris, A. Shukla and J.L. Margrave, 2003. Adsorption of chromium from aqueous solutions by maple sawdust, J. Hazard. Mater., B 100: 53-63.
26. Shukla, A., Y.H. Zhang, P. Dubey, J.L. Margrave and S.S. Shukla, 2002. The role of sawdust in the removal of unwanted materials from water, J. Hazard. Mater., B 95: 137-152.
27. Kumar, P.S., S. Ramalingam, C. Senthamarai, M. Niranjanaa, P. Vijayalakshmi and S. Sivanesan, 2010. Adsorption of dye from aqueous solution by cashew nut shell: studies on equilibrium isotherm, kinetics and thermodynamics of interactions, Desalination, 261: 52-60.
28. Li, Y., J. Zhang, C. Zhang, L. Wang and B. Zhang, 2008. Biosorption of methylene blue from aqueous solution by softstem bulrush (*Scirpus tabernaemontani* Gmel.), J. Chem. Technol. Biotechnol., 83: 1639-1647.
29. Han, R., W. Zou, W. Yu, S. Cheng, Y. Wang and J. Shi, 2007. Biosorption of methylene blue from aqueous solution by fallen phoenix tree's leaves, J. Hazard. Mater., 141: 156-162.
30. Lagergren, S., 1898. Zur theorie der sogenannten adsorption gelöster stoffe. Kungliga Svenska Vetenskapsakademiens, Handlingar, 24: 1-39.
31. Ho, Y.S. and G. McKay, 1999. Pseudo-second order model for sorption processes, Process Biochem., 34: 450-465.
32. Weber, W.J. and J.C. Morris, 1963. Kinetics of adsorption on carbon from solution, J. Sanit. Eng. Div. ASCE 89: 31-59.
33. Bhatnagar, A. and A.K. Minocha, 2010. Biosorption optimization of nickel removal from water using Punica granatum peel waste, Colloids Surf., B, 76: 544-548.
34. Wang, L., J. Zhang, R. Zhao, C. Li, Y. Li and C.L. Zhang, 2010. Adsorption of basic dyes on activated carbon prepared from Polygonum orientale Linn: equilibrium, kinetic and thermodynamic studies, Desalination, 254: 68-74.

35. Langmuir, I., 1918. The adsorption of gases on plane surfaces of glass, mica and platinum, J. Am. Chem. Soc., 40(9): 1361-1403.
36. Freundlich, H., 1906. Over the adsorption in the solution, J. Phys. Chem., 57: 385-470.
37. Al-Anber, Z.A., A.M. Al-Anber, M. Matouq, O. Al-Ayed and N.M. Omari, 2011. Defatted Jojoba for the removal of methylene blue from aqueous solution: Thermodynamic and kinetic studies, Desalination 276: 169-174.